



# Generation of Brønsted acidity in AlMCM-41 by sulphation for enhanced liquid phase *tert*-butylation of phenol

Eng-Poh Ng<sup>\*</sup>, Hadi Nur<sup>\*\*</sup>, Ka-Lun Wong, Mohd Nazlan Mohd Muhid, Halimatun Hamdan

*Ibnu Sina Institute for Fundamental Science Studies, Universiti Teknologi Malaysia, 81310 UTM Skudai, Johor, Malaysia*

Received 7 December 2006; received in revised form 26 January 2007; accepted 1 February 2007

Available online 6 February 2007

## Abstract

AlMCM-41 mesoporous molecular sieve modified by impregnation with sulphuric acid in toluene possesses only Brønsted acid sites. The catalyst exhibits a high catalytic activity for *tert*-butylation of phenol with high selectivity to 2,4-di-*tert*-butylphenol in liquid phase. <sup>27</sup>Al MAS NMR study indicates that the modification of AlMCM-41 with sulphuric acid in toluene leaves only octahedrally coordinated Al species. The tetrahedrally coordinated Al species which exist before modification with sulphuric acid in toluene being dealuminated to form extraframework octahedrally coordinated Al species. The mesoporous structure of AlMCM-41 is retained after modification, but pore size decreases by ca. 3 Å by the modification. The active sites are postulated on the basis of XRD, FTIR, <sup>27</sup>Al MAS NMR, TGA, BET analysis and FTIR-pyridine adsorption studies that –OSO<sub>3</sub>H bonded to octahedrally coordinated Al species.

© 2007 Elsevier B.V. All rights reserved.

**Keywords:** Sulphation; AlMCM-41; Brønsted acid; *tert*-Butylation; Phenol

## 1. Introduction

The recent discovery of well-ordered mesoporous MCM-41 has opened a new field in advanced material research [1]. This material has a very high surface area and pore diameter that can be tailored from 20 to 100 Å, making it a promising candidate as catalysts and supports [1]. However, there is no acidity in purely siliceous MCM-41. It has been reported that Brønsted acid site can be created by incorporation of metal such as aluminum into their framework [2] or via post-synthesis modifications [3]. However, such method is limited in producing moderate Brønsted acid strength [2]. Therefore, a demand for enhancing the acidity is needed to overcome this problem. Recently, several researchers [4–7] have reported the sulphation on the surface of AlMCM-41 and TS-1 materials to improve their catalytic activity. They reported that sulphation leads to produce only Lewis acidity. Most recently, we reported a new approach to produce Brønsted acidity in AlMCM-41 by

sulphation method [7]. The approach is based on the idea that the acidity formed is influenced by the use of hydrophobic solvent so that it can protect the sulphate group from being hydrolyzed and produce Brønsted acid sites. We have also demonstrated that sulphated AlMCM-41 catalyst prepared by sulphation catalyzes dibenzoylation of biphenyl [8]. In the present study, we examined the physicochemical properties of sulphated AlMCM-41 in more detail and evaluated its catalytic activity in liquid phase *tert*-butylation of phenol.

Liquid phase *tert*-butylation of phenol has been studied extensively because it is widely used in the production of antioxidant intermediates, phenolic resins, heat stabilizers of polymeric materials, fragrances, oil field chemicals and demulsifiers [9,10]. In general, this reaction is catalyzed by conventional homogeneous acid catalysts such as Brønsted acids (H<sub>2</sub>SO<sub>4</sub>, HF, H<sub>3</sub>PO<sub>4</sub> and HClO<sub>4</sub>) and Lewis acids (AlCl<sub>3</sub> and BF<sub>3</sub>) [11]. However, these catalysts are environmentally unfriendly, unselective and require tedious work-up. Usually, *tert*-butylation of phenol using zeolitic catalysts is carried out in vapour phase. Vapour phase *tert*-butylation of phenol over zeolitic catalysts produced *ortho*, *meta*, *para*, *ortho-ortho* and *ortho-para* di-*tert*-butylated products [10,12–18]. The reaction requires higher temperature (>140 °C) to be carried out. This reaction has not been studied intensively using solid acid catalyst

\* Corresponding author. Tel.: +60 12 742 1053.

\*\* Corresponding author.

E-mail addresses: [engpoh81@yahoo.com.au](mailto:engpoh81@yahoo.com.au) (E.-P. Ng), [hadi@kimia.fs.utm.my](mailto:hadi@kimia.fs.utm.my) (H. Nur).

at low temperature [19,20]. In this paper, liquid phase *tert*-butylation of phenol with methyl tertiary butyl ether (MTBE) at low temperature in the presence of sulphated AIMCM-41 is demonstrated. For comparison, the activity of some solid and liquid acid catalysts, such as HZSM-5, H<sub>2</sub>SO<sub>4</sub>, tungstophosphoric acid (HPW) and HAIMCM-41 were also studied.

## 2. Experimental

### 2.1. Synthesis of AIMCM-41

AIMCM-41 with SiO<sub>2</sub>/Al<sub>2</sub>O<sub>3</sub> = 15 and 80 were prepared in the following way using published method [21]. In a typical synthesis, sodium silicate (Na<sub>2</sub>SiO<sub>3</sub>) was prepared by combining rice husk ash (6.13 g, 97% SiO<sub>2</sub>) with NaOH pellet (2.00 g, Merck 99%) and H<sub>2</sub>O (40.0 ml, double distilled). The resulting gel mixture was heated and stirred for 2 h at 90 °C. The resulting solution was labeled as solution A. Another solution B was prepared by mixing appropriate amount of NaAlO<sub>2</sub> (Riedel-de-Haän<sup>®</sup>, 50–56% Al<sub>2</sub>O<sub>3</sub>), 6.07 g of CTABr and 0.70 g of NH<sub>4</sub>OH 25 wt.% in 35 ml distilled water, followed by stirring at 80 °C until a clear solution was obtained. For the samples with SiO<sub>2</sub>/Al<sub>2</sub>O<sub>3</sub> ratio = 15 and 80, 1.277 g and 0.239 g of NaAlO<sub>2</sub> were added into the solution, respectively. After that, both solutions A and B were mixed together in a polypropylene bottle to give a gel with a composition of 6SiO<sub>2</sub>:CTABr:1.5Na<sub>2</sub>O:xAl<sub>2</sub>O<sub>3</sub>:0.15(NH<sub>4</sub>)<sub>2</sub>O:250H<sub>2</sub>O. The resulting gel was vigorously stirred for 15 min and kept in an air oven for crystallization at 100 °C for 24 h. The gel mixture was then cooled to room temperature and the pH of the reaction mixture was adjusted to pH 10.2 by drop wise addition of 25 wt.% acetic acid (Merck) with vigorous stirring. The subsequent 24 h heating and pH adjustment was repeated twice. The final product was filtered, washed, dried and calcined at 550 °C in air for 10 h with a heating rate of 1 °C min<sup>-1</sup>.

### 2.2. Preparation of HAIMCM-41 and sulphated AIMCM-41

Calcined MCM-41 mesoporous materials (0.700 g) in Na<sup>+</sup> form was put into a 50 ml of 0.2 M NH<sub>4</sub>NO<sub>3</sub> solution and stirred at 60 °C for 6 h. The solid was filtered, washed with deionized water and dried at 110 °C for 2 h. The ion exchange was repeated three times. The solid powder was then calcined at 550 °C for 5 h. The solid powders of H-AIMCM41 with SiO<sub>2</sub>/Al<sub>2</sub>O<sub>3</sub> ratio of 15 and 80 were labeled as H-15 and H-80, respectively. The sulphated AIMCM-41 was prepared by impregnating 30 μl H<sub>2</sub>SO<sub>4</sub> (95–97%, 0.56 mmol) sulphuric acid on AIMCM-41 in 10 ml of toluene. Then the sample was stirred at 50 °C for 1.0 h and dried at 130 °C for 12 h. The sulphated AIMCM-41 with SiO<sub>2</sub>/Al<sub>2</sub>O<sub>3</sub> ratios of 15 and 80 were labeled as S-15 and S-80, respectively.

### 2.3. Catalysts characterization

The XRD patterns of powdered MCM-41 samples were recorded between 1.5° and 10.0° 2θ with a Bruker Advance D8

using Siemens 5000 diffractometer with Cu Kα radiation operating at λ = 1.5418 Å, 40 kV, 40 mA. The FTIR spectra were recorded using a Perkin-Elmer Spectrum One FTIR spectrometer with a resolution of 4 cm<sup>-1</sup> and 10 scans in the mid IR region (400–4000 cm<sup>-1</sup>). Micromeritics ASAP 2010 volumetric adsorption analyzer was used to measure the N<sub>2</sub> adsorption–desorption isotherms of the samples. Prior to the measurements, the samples were degassed at 200 °C overnight. The data were acquired automatically by the computer program. TGA measurements were recorded by using a Mettler Toledo TGA/SDTA851 Thermogravimetric/Differential Thermal Analyzer at a heating rate of 10 °C/min, from room temperature to 800 °C in an air flow of 20 ml/min. <sup>27</sup>Al MAS NMR spectra were recorded on a Bruker Avance 400 MHz spectrometer at a frequency of 104.2 MHz with a spin rate of 7 kHz, pulse length of 1.9 μs, relaxation time delay of 2 s and 5000 scans. The chemical shifts of <sup>27</sup>Al were reported in relation to Al(H<sub>2</sub>O)<sup>3+</sup>. IR spectra of adsorbed pyridine were recorded to determine the presence of Brønsted and Lewis acid sites over the catalysts. A self-supporting wafer (15 mg) of the sample was preheated at 200 °C for 2 h under vacuum (10<sup>-6</sup> mbar) before adsorbing an excess of pyridine at room temperature, followed by desorption at 150 and 350 °C. All the spectra were recorded with a 4 cm<sup>-1</sup> resolution and 10 scans in the range of 1650–1440 cm<sup>-1</sup>.

### 2.4. Catalytic tests

*tert*-Butylation of phenol whereby phenol (4 mmol), MTBE (4 mmol) and 0.5 g of activated catalyst were added to a refluxed and magnetically stirred round bottom flask (50 ml) under atmospheric pressure containing hexadecane (30 μl) and nitrobenzene (10 ml) as internal standard and solvent, respectively, at 110 °C. Catalyst was activated at 200 °C for 2 h before conducting reaction in order to remove adsorbed water vapor. The products were analyzed by GC–MS (Agilent 6890N-5973 Network Mass Selective Detector) equipped with HP-5MS column (30 m × 0.251 mm × 0.25 μm). The products were also periodically withdrawn and analyzed by GC (ThermoFinnigan's Chrom-Card S/W for Trace/Focus<sup>TM</sup> GC) equipped with a flame ionization detector (FID) and a non-polar capillary column (Equity 1). The same procedures were also performed for other catalysts where 0.5 g of solid acid catalyst and 0.56 mmol of homogeneous catalysts were used. Besides, the other solvents (10 ml) with different polarity such as dodecane and chlorobenzene were used to study the effect of solvent. Apart from that, phenol: MTBE ratio = 1:1, 1:3 and 1:6 were used in order to study the effect of MTBE loading.

### 2.5. Leaching test

In order to check the possible leaching, sulphated AIMCM-41 was suspended in nitrobenzene. After the mixture was stirred for 6 h at 110 °C, the suspension was centrifuged to separate the solid catalyst. The reaction was performed after washing and drying of the catalyst with hexadecane, phenol (4 mmol) and

MTBE (4 mmol) under reflux at 110 °C for 6 h. The reaction solution was then taken out and analyzed by GC.

### 3. Results and discussion

#### 3.1. Physical properties

The XRD patterns of protonated and sulphated AIMCM-41 are shown in Fig. 1. As displayed in the figure, the samples exhibit an intense signal at about  $2\theta = 2.2^\circ$  due to (1 0 0) plane and weak signals between  $3.5^\circ$  and  $6.0^\circ$  due to (1 1 0) and (2 0 0) planes. These peaks are typical of MCM-41 materials which confirm the hexagonal mesophase of the materials [1]. Meanwhile, a typical XRD pattern after sulphation of AIMCM-41 showed weaker peaks of (1 0 0), (1 1 0) and (2 0 0) planes indicating that the long range order of AIMCM-41 has decreased after the modification. However, as shown in Table 1, a decrease of the value of  $d$ -spacing and unit cell parameter was observed indicating a decrease in pore diameter of AIMCM-41 due to the incorporation of sulphate groups. This suggests that sulphate groups have been successfully immobilized in the pore of MCM-41.

The results from Table 1 also infer that the pore volume and pore diameter of the series of sulphated AIMCM-41 decrease in both surface area and pore volume in comparison to that of protonated AIMCM-41. The changes in pore volume and surface area may be due the decomposition of pore structure of AIMCM-41 and it is in line with the results of XRD analysis. Apart from that, further investigation also reveals that the pore diameter decreases steadily for the sulphated samples with increment in aluminum content. The shrinkage of pore diameter might be due to dealumination process to produce extraframework aluminum (EFAL) which reacts with sulphate ion. One

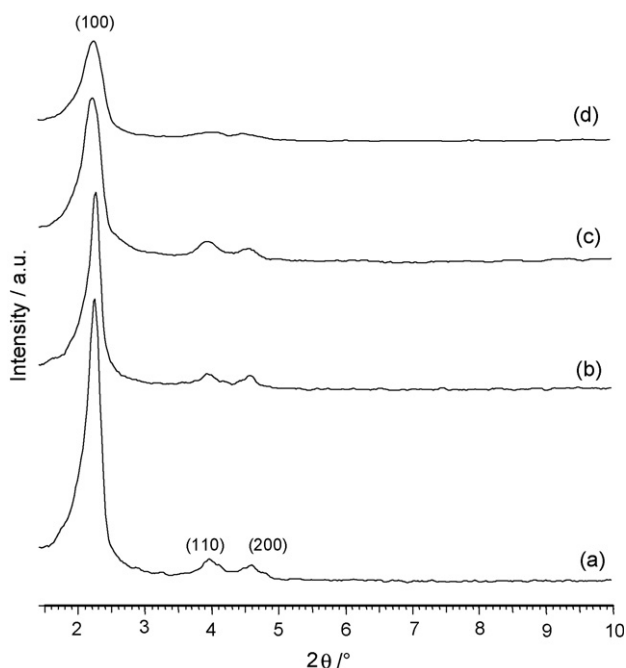


Fig. 1. X-ray diffractogram patterns of: (a) H-80, (b) H-15, (c) S-80 and (d) S-15.

expects that these sulphated aluminum species will cover the surface of the pore, leading to reduction of pore diameter and pore volume as illustrated in Fig. 2. Additionally, pore diameter and pore volume shrinkages are also owing to reaction between the sulphate groups with the surface silanol groups. In our previous results, it has been proven that sulphate groups not only react with aluminum but also surface silanol group [8]. Hence, the pore diameter will become smaller as more sulphated aluminum and silicon species are in the sample. Meanwhile, the pore wall thickness for all protonated samples remains fairly constant. However, its thickness increases after sulphation. It may be due to coverage of sulphated aluminum species on the pore walls, leading to increment in pore wall thickness.

Table 1 also shows the acidity of protonated and sulphated AIMCM-41 with various  $\text{SiO}_2/\text{Al}_2\text{O}_3$  ratios. Both H-80 and H-15 samples exhibit two types of acid site: Brönsted acid and Lewis acid sites which gave peaks at 1546 and 1455  $\text{cm}^{-1}$  in their pyridine-FTIR spectra, respectively. It can also be seen that increment in aluminum content in protonated AIMCM-41 leads to increment of the amount of Brönsted and Lewis acid sites. However, this trend is different in sulphated AIMCM-41 samples. Sulphated AIMCM-41 materials possess only Brönsted acid site since there is no peak at  $\sim 1455 \text{ cm}^{-1}$ . Moreover, sulphated AIMCM-41 (S-80) with lower aluminum content shows the highest amount of Brönsted acid sites compared to that of S-15. When this result is combined with the  $^{27}\text{Al}$  MAS NMR data, it shows that Brönsted acid in sulphated MCM-41 is attributed to octahedrally coordinated aluminum since the peak for tetrahedral aluminum was not observed in  $^{27}\text{Al}$  MAS NMR spectra (see Fig. 7). This phenomenon is supported by the pyridine-FTIR spectra of protonated and sulphated AIMCM-41 at different temperature. It is clear from Table 1 that as the desorption temperature is increased, the amount of Brönsted acid site in sulphated AIMCM-41 is still higher than that of protonated AIMCM-41 (H15 and H80). This suggests the existence of strong Brönsted acid sites in sulphated AIMCM-41 whereby it is required in obtaining di-*tert*-butylation products [18].

Fig. 3 shows the nitrogen adsorption–desorption isotherms of protonated and sulphated AIMCM-41. The nitrogen adsorption–desorption isotherms of both types of samples possess the typical irreversible type IV adsorption isotherm with type H4 hysteresis loop in accordance with IUPAC recommendations [23]. It shows that the resultant MCM-41

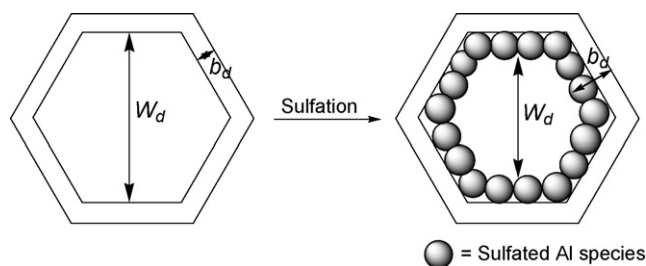


Fig. 2. Modification of surface of MCM-41 through sulphation leads to shrinkage of pore diameter.

Table 1  
The physical and acidity properties of various forms of AlMCM-41 samples

Samples	$d_{100}$ spacing (Å)	$a_0$ (Å)	BET surface area ( $\text{m}^2 \text{g}^{-1}$ )	Pore volume, $V_p$ ( $\text{cm}^3 \text{g}^{-2}$ )	Pore wall thickness, $b_d$ (Å)	Pore diameter, $W_d$ (Å) <sup>a</sup>	Acidity <sup>b</sup> ( $\mu\text{mol g}^{-1}$ )			
							Brönsted		Lewis	
							150 °C	350 °C	150 °C	350 °C
H-80	37.5	43.6	803	0.7	9.5	35.9	19.4	8.9	36.6	25.7
H-15	38.2	44.1	791	0.7	9.4	36.4	23.2	11.8	43.1	33.4
S-80	37.2	43.0	538	0.5	11.7	32.8	110.2	13.7	0	0
S-15	37.9	43.8	499	0.5	12.7	32.6	98.9	18.5	0	0

<sup>a</sup> The values were calculated from the formulae in [22].

<sup>b</sup> The amount of Brönsted and Lewis acid sites were determined by the pyridine-FTIR spectroscopy after the samples were evacuated at 150 and 350 °C. The Brönsted and Lewis acid sites gave peaks at 1546 and 1455  $\text{cm}^{-1}$ , respectively.

materials possess uniform slit-shaped mesopores. The adsorption isotherm of S-80 and S-15 exhibits a sharp inflection at relative pressures of  $0.20 < P/P_0 < 0.35$ , which corresponds to capillary condensation of nitrogen inside the mesopores [24]. The isotherm was followed with a plateau with a slight inclination at high relative pressures which is due to multilayer adsorption on the surface of the sample. However, the protonated samples exhibit higher and steeper capillary condensation step than that of the sulphated samples. There is also a marked decrease in volume adsorbed for sulphated AlMCM-41 samples. This strongly suggests that sulphate groups have been successfully immobilized in the pore of MCM-41, resulting in reduction of pore volume as discussed previously.

The infrared spectra of the protonated and sulphated AlMCM-41 molecular sieves are presented in Fig. 4. The

broad peak around  $3417 \text{ cm}^{-1}$  is due to O–H stretching of water and the peak at around  $1638 \text{ cm}^{-1}$  corresponds to bending mode of O–H of water. Besides those, the peaks around 1288 and  $1180 \text{ cm}^{-1}$  are attributed to the asymmetric stretching of Si–O–Si groups. The symmetric stretching modes of Si–O–Si groups are observed at around 806 and  $580 \text{ cm}^{-1}$ . The peak at  $963 \text{ cm}^{-1}$  is assigned to the presence of defective Si–OH groups while the adsorption band at  $458 \text{ cm}^{-1}$  is assigned to bending vibration of Si–O–Si or Al–O–Si groups. Some additional peaks; stretching vibration of  $\text{HSO}_4^-$  at 883 and  $580 \text{ cm}^{-1}$  and asymmetric stretching of the S=O bond at  $1288 \text{ cm}^{-1}$  confirm the presence of sulphate in sulphated AlMCM-41 [4,25].

Fig. 5 shows the thermograms of protonated AlMCM-41 (H-80) and sulphated AlMCM-41 (S-80). Both samples show a remarkable weight loss below 200 °C due to desorption of

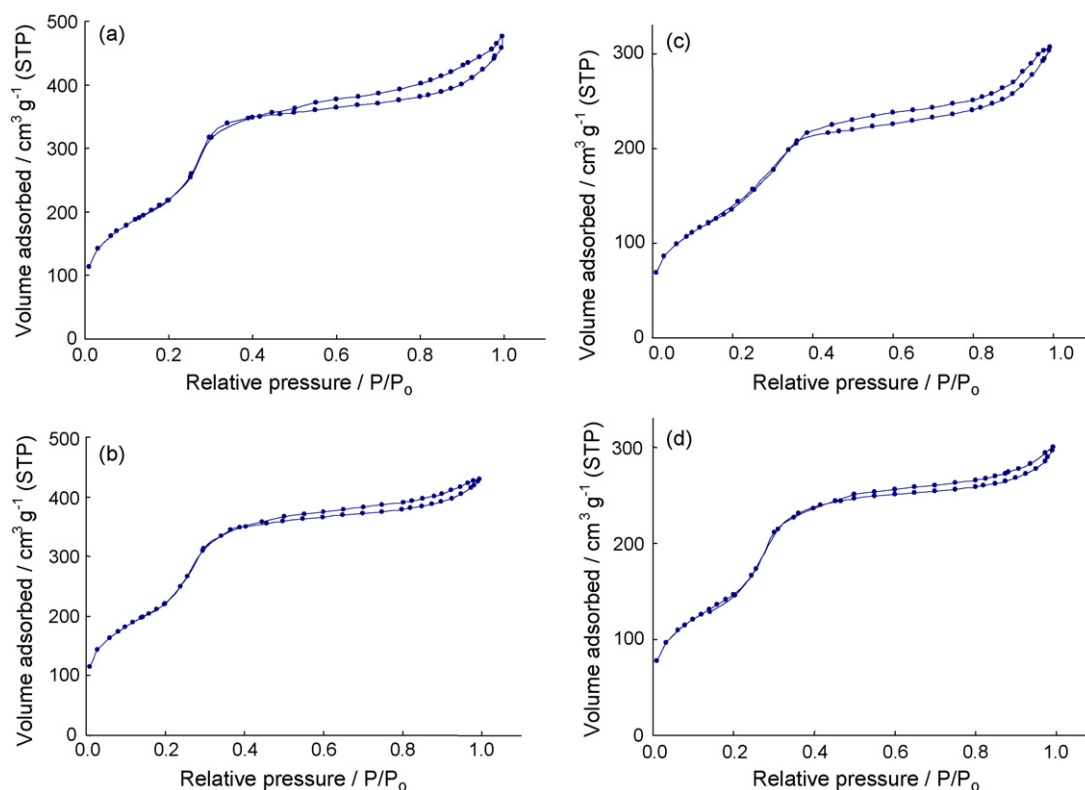


Fig. 3. Nitrogen adsorption–desorption isotherms of: (a) H-80, (b) H-15, (c) S-80 and (d) S-15.

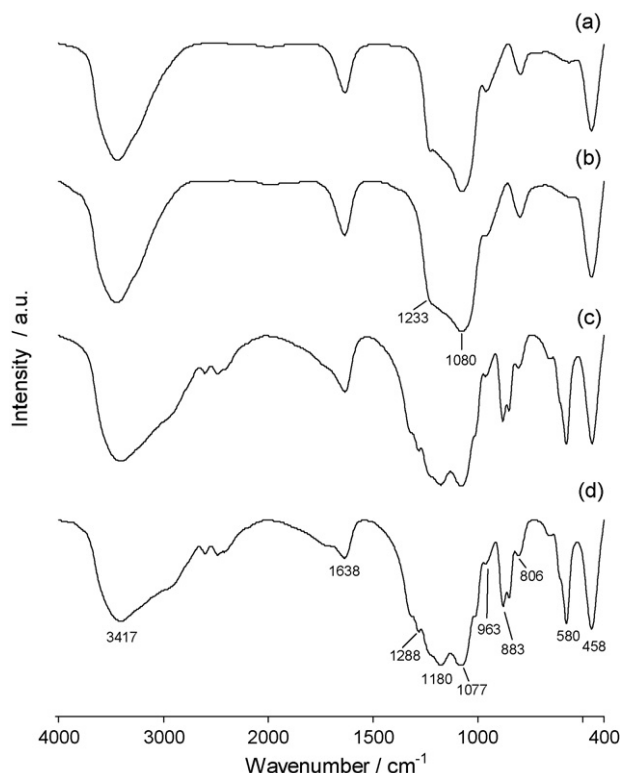


Fig. 4. Infrared spectrum of: (a) H-80, (b) H-15, (c) S-80 and (d) S-15.

water and a slight weight loss above 200 °C due to thermal condensation of silanol groups. It can be observed that the thermogram of S-80 taken in air exhibits one additional stage of weight loss; 300–800 °C, which corresponds to the decomposition of sulphate groups attached on the surface of MCM-41. From the data obtained, H-80 followed two steps of weight loss whereas the S-80 involved three steps of weight loss, verifying that the sulphate groups had successfully attached to the surface of MCM-41.

Fig. 6 shows the  $^{27}\text{Al}$  MAS NMR spectra of H-80 and H-15 samples. The spectra of both samples show two intense signals at 54 and 0 ppm which correspond to the tetrahedral aluminum in the framework structure and octahedrally coordinated extraframework aluminums (EFAL), respectively [20]. The intensity of both peaks increases as the aluminum content increases. Conventionally, Lewis acid is attributed to the octahedrally coordinated aluminums while the Brönsted acid is attributed to framework tetrahedrally coordinated aluminum. It

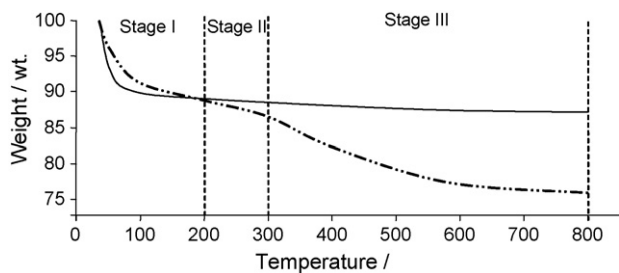


Fig. 5. Thermogravimetric analysis of: (a) H-80 and (b) S-80 samples in nitrogen gas flow with 10 °C/min heating rate.

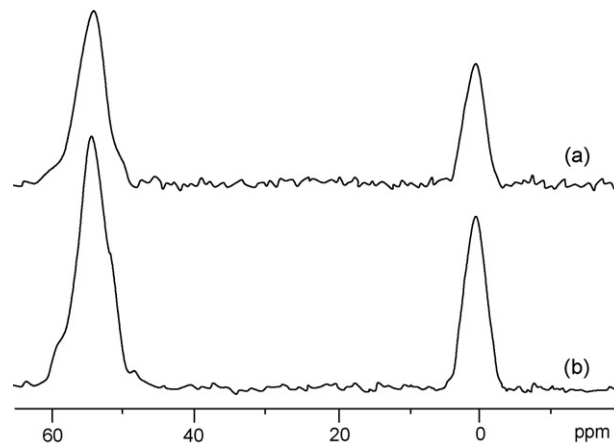


Fig. 6.  $^{27}\text{Al}$  MAS NMR spectra of: (a) H-80 and (b) H-15.

can be inferred that the results acquired by  $^{27}\text{Al}$  MAS NMR and pyridine-FTIR spectroscopies for H-80 and H-15 are compatible.

However, in the case of sulphated AIMCM-41, the conventional rule contradicts with the results obtained because the spectra of S-80 and S-15 shown in Fig. 7 reveal the presence of only two peaks at 0 and –5 ppm which are assigned to two types of octahedrally coordinated aluminums. Since the  $^{27}\text{Al}$  MAS NMR study does not reveal the presence of the peak for tetrahedral aluminum, the Brönsted acidity must be due to the introduction of hydrogen sulphate group ( $-\text{OSO}_3\text{H}$ ) into the sample that may have formed bonds with the octahedral aluminum. The disappearance of the peak corresponding to tetrahedral aluminum indicates that after treatment with sulphuric acid, tetrahedrally coordinated aluminum was dealuminated from the framework and transformed to octahedral aluminum; generally referred to as extraframework aluminum (EFAL). After detail examination of spectra of S-80 and S-15, it can be suggested that a strong peak at 0 ppm corresponds to octahedral Al in  $\text{Al}_2(\text{SO}_4)_3$  [26] and another peak at around –5 ppm is due to octahedral Al in sulphated Al species [8].

Generation of Brönsted acidity instead of Lewis acidity by sulphation seems unusual because previously it has been reported that the sulphation generates only Lewis acidity [4–7]. Although the mechanism of generation of Brönsted acid sites in

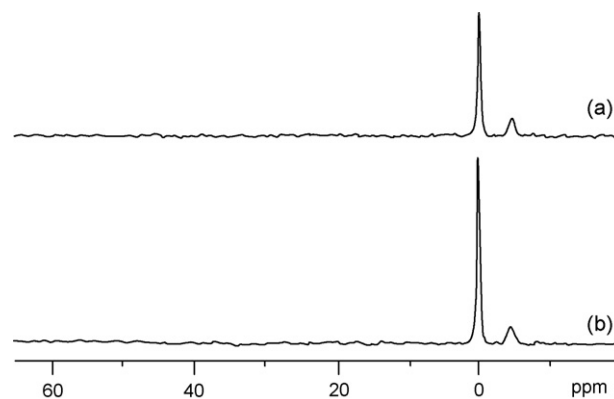


Fig. 7.  $^{27}\text{Al}$  MAS NMR spectra of: (a) S-80 and (b) S-15.

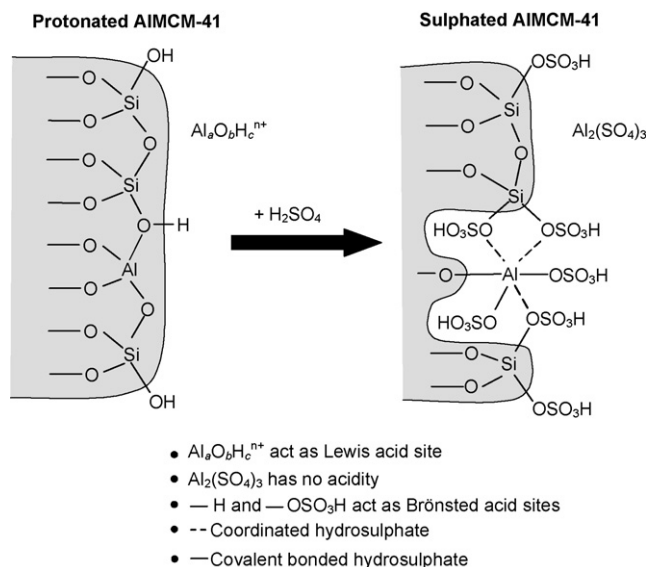


Fig. 8. The possible structure of sulphated AIMCM-41.

sulphated AIMCM-41 has not yet been clearly understood, this phenomenon could be explained in term of the use of hydrophobic solvent during the sulphation of AIMCM-41. The sulphate groups attached to the AIMCM-41 would be hydrolyzed in hydrophilic solvent such as water to produce Lewis acid sites. However, hydrophobic organic solvent such as dehydrated toluene could protect sulphate groups from being hydrolyzed and hence produce Brönsted acid sites. The alternative explanation is that the possibility of the formation of *p*-toluenesulfonic acid (TsOH), a strong organic acid, through sulphonation of toluene. It is possible that the TsOH react with tetrahedrally coordinated Al species and protect it from being hydrolyzed to produce Lewis acid site. However, the existence of TsOH cannot be detected due to its trace amount in the solid catalyst.

Based on the above considerations and experimental results, a model of the sulphated AIMCM-41 with Brönsted acid sites is proposed (see Fig. 8). The Lewis acid sites in HAIMCM-41 originated from extraframework Al species (EFAL) present in the form of  $\text{Al}^{3+}$ ,  $\text{AlO}^+$ ,  $\text{Al}(\text{OH})_2^+$ ,  $\text{Al}(\text{OH})_2^{2+}$  or charged  $\text{Al}_x\text{O}_y\text{H}_c^{n+}$  cluster within the sample where they are represent as  $\text{Al}_x\text{O}_y\text{H}_c^{n+}$  [27]. One considers that the sulphuric acid would react with Si–OH and Al–OH, leading to migration of Al atom to extraframework to produce  $\text{Al}_2(\text{SO}_4)_3$  which has no acidity. It is proposed that the Brönsted acid site is created through attack of two anions of  $-\text{OSO}_3\text{H}$  (strong nucleophile) to Al atom to form trivalent Al followed by stabilization of Al atom with octahedral coordination through covalent with hydrogen sulphate ( $-\text{OSO}_3\text{H}$ ) groups which are attached to Si atoms (see Fig. 8).

### 3.2. Catalytic activity for *tert*-butylation of phenol

The activity of S-80 and S-15 catalysts were tested in *tert*-butylation reaction of phenol. The effect of temperature towards *tert*-butylation of phenol under batch and atmospheric

Table 2

Phenol conversion over sulphated AIMCM-41 as catalysts<sup>a</sup>

Catalysts	Phenol conversion (%)	Selectivity (%)			
		2-TBP <sup>b</sup>	4-TBP <sup>c</sup>	2,4-DTBP <sup>d</sup>	2,6-DTBP <sup>e</sup>
S-15	52.0	40.3	33.5	26.3	0.0
S-80	59.7	39.2	29.7	31.1	0.0

<sup>a</sup> The reactions were carried out at 110 °C for 6 h with the molar ratio of phenol to MTBE was 1:1.

<sup>b</sup> 2-*tert*-Butylphenol.

<sup>c</sup> 4-*tert*-Butylphenol.

<sup>d</sup> 2,4-di-*tert*-Butylphenol.

<sup>e</sup> 2,6-di-*tert*-Butylphenol.

pressure conditions was studied at 110 °C. Table 2 tabulates the conversion and selectivity of products after 6 h of reaction. S-15 and S-80 were able to convert 52.0 and 59.7% of phenol, respectively. It can also be observed that S-80 was more active than S-15 due to the higher amount of acid site in S-80 than in S-15 (see Table 1).

The influences of the molar ratio of phenol to MTBE on the activity and selectivity of S-80 were also studied at 110 °C. Table 3 tabulates the phenol conversion and product selectivity of the reaction using the molar ratio of phenol to MTBE are 1:1, 1:3 and 1:6. It is clear that an increase in the conversion of phenol and selectivity to 2,4-DTBP was observed with the decrease in phenol to MTBE molar ratio. However, a decrease in conversion and selectivity to 2,4-DTBP was observed when the molar ratio of phenol to MTBE equals to 1:6 was used. Besides, no product was observed when MTBE was used as solvent in the reaction. It was found that the reaction system with molar ratio of phenol:MTBE = 1:3 is the most suitable condition for di-*tert*-butylation of phenol over S-80.

In order to study the effect of solvent towards the activity of *tert*-butylation of phenol, several solvents with different polarity measured with  $E_T^N$  such as nitrobenzene ( $\text{PhNO}_2$ ), chlorobenzene ( $\text{PhCl}$ ) and dodecane ( $\text{C}_{12}\text{H}_{26}$ ) were used as reaction solvent. Results from Table 4 indicate that the activity of the catalyst in *tert*-butylation of phenol is higher when a low polar solvent (e.g.  $\text{C}_{12}\text{H}_{26}$ ) is used. This might be due to the occurrence of competitive adsorption between reactant and solvent on the surface of catalyst. Theoretically, highly polarizable molecules (e.g.  $\text{PhNO}_2$ ) can interact stronger with the surface of catalyst via hydrogen bonding or electron donation [28]. Such interaction can poison the rate of adsorption–desorption rate of reactant that will slower the alkylation process. Low polarizable molecules (e.g.  $\text{C}_{12}\text{H}_{26}$ ),

Table 3

Effect of the molar ratio of phenol to MTBE on phenol conversion<sup>a</sup>

Phenol:MTBE ratio	Phenol conversion (%)	Selectivity (%)			
		2-TBP	4-TBP	2,4-DTBP	2,6-DTBP
1:1	59.7	39.2	29.7	31.1	0.0
1:3	68.1	19.2	21.2	59.6	0.0
1:6	47.3	54.3	19.1	21.3	5.4

<sup>a</sup> The reactions were carried out at 110 °C for 6 h over S-80 catalyst with the molar ratio of phenol to MTBE was 1:1.

Table 4  
Effect of solvent on phenol conversion<sup>a</sup>

Solvents	Polarity ( $E_T^N$ )	Phenol conversion (%)	Selectivity (%)			
			2-TBP	4-TBP	2,4-DTBP	2,6-DTBP
PhNO <sub>2</sub>	0.324	59.7	39.2	29.7	31.1	0.0
PhCl	0.188	68.6	55.4	21.9	22.4	0.4
C <sub>12</sub> H <sub>26</sub>	0.012	79.9	26.5	49.5	24.0	0.0

<sup>a</sup> Reaction conditions are the same as those given for Table 3.

however, can only weakly interact with active sites of catalyst via induced dipoles and hence do not affect the adsorption–desorption rate as occur in PhNO<sub>2</sub> and PhCl. As a result, the reaction favourably occurs in non-polar solvent. As tabulated in Table 4, the reaction rate or activity of the catalyst for the solvent with different polarity is found to be in the following order: PhNO<sub>2</sub> < PhCl < C<sub>12</sub>H<sub>26</sub>.

Table 5 summarizes the results of *tert*-butylation of phenol over various types of catalysts; HZSM-5 (SiO<sub>2</sub>/Al<sub>2</sub>O<sub>3</sub> = 30), H<sub>2</sub>SO<sub>4</sub>, tungstophosphoric acid (HPW) and HAIMCM-41 (H-80). It is interesting to note that HZSM-5 gave very small conversion of phenol (12.0%) due to small channel structure [11], making the reactants and products have difficulty to diffuse effectively in the pore of zeolite HZSM-5. Therefore, the reaction was only able to be catalyzed by the acid sites located on the external surface of HZSM-5. On the other hand, large mesoporous materials such as HAIMCM-41 (H-80) and sulphated AIMCM-41 (S-80) are beneficial in catalyzing this reaction. The occurrence of such phenomenon might be due to the effect of surface polarity of the support. It is known that the sulphate (–OSO<sub>3</sub><sup>–</sup>) anion is a polar group. The existence of this anion on the surface of sulphated AIMCM-41, makes it more polar and hydrophilic than HAIMCM-41. As a consequence, the polar reactant such as phenol tends to be attracted to the surface and is activated to undergo *tert*-butylation reaction. It is revealed that the activity of concentrated sulphuric acid and HPW is comparable to those of sulphated AIMCM-41, giving 59.7% conversion of phenol but less selective to 2,4-DTBP, indicating that the amount or/and strong acid sites in sulphuric acid and HPW are not comparable in producing disubstituted 2,4-DTBP. This suggests that the generation of Brønsted acidity in AIMCM-41 by sulphation plays an important role for enhanced liquid phase *tert*-butylation of phenol in producing

Table 5  
Effect of catalyst on phenol conversion<sup>a</sup>

Catalysts	Phenol conversion (%)	Selectivity (%)			
		2-TBP	4-TBP	2,4-DTBP	2,6-DTBP
H <sub>2</sub> SO <sub>4</sub> <sup>a,b</sup>	63.3	24.8	53.6	13.8	7.8
HPW <sup>b,c</sup>	59.2	7.0	81.6	3.0	8.4
HZSM-5 <sup>d</sup>	12.0	75.0	25.0	0.0	0.0
S-80	59.7	39.2	29.7	31.1	0.0
H-80	45.1	59.5	26.9	13.7	0.0

<sup>a</sup> Reaction conditions are the same as those given for Table 4.

<sup>b</sup> Homogeneous catalyst.

<sup>c</sup> HPW, tungstophosphoric acid.

<sup>d</sup> SiO<sub>2</sub>/Al<sub>2</sub>O<sub>3</sub> ratio = 30.

disubstituted products. Hence, the study indicates that sulphated AIMCM-41 is a promising candidate as a catalyst for acidic catalytic reaction such as di-*tert*-butylation of phenol that requires strong and large amount of acid sites.

Leaching is a particular problem of solid catalysts in liquid-phase reaction especially when polar or protic solvents are used [29]. The activities of the recovered and dried sulphated AIMCM-41 were negligible when nitrobenzene; a polar solvent was used in the leaching test at 110 °C. This strongly suggests that the sulphate groups are chemically bonded to the mesoporous support and it agrees with the result obtained by thermogravimetry analysis.

#### 4. Conclusions

Sulphated AIMCM-41 with different SiO<sub>2</sub>/Al<sub>2</sub>O<sub>3</sub> ratios was synthesized using impregnation of sulphuric acid in organic solvent and its physicochemical properties were intensively investigated. From the results of <sup>27</sup>Al NMR and pyridine-FTIR spectroscopies, it was found that sulphated AIMCM-41 contains octahedral aluminum with Brønsted acidity. The results reveal that sulphated AIMCM-41 shows a good activity in *tert*-butylation of phenol with MTBE at 110 °C. The results also show that the sulphated sample with higher SiO<sub>2</sub>/Al<sub>2</sub>O<sub>3</sub> ratio gave higher activity towards *tert*-butylation of phenol whereas non-polar solvent (C<sub>12</sub>H<sub>26</sub>) is beneficial in increasing the activity of sulphated AIMCM-41 in *tert*-butylation of phenol. Since the activity of sulphated AIMCM-41 is comparable with concentrated sulphuric acid and HPW, one considers that the hydrophilic nature and the ordered structure of sulphated AIMCM-41 may contribute to high activity and selectivity in *tert*-butylation of phenol. It is revealed that sulphated AIMCM-41 faces negligible leaching problem which offers another environmentally friendly replacement for conventional acidic catalyst.

#### Acknowledgement

The authors would like to acknowledge the Ministry of Science, Technology and Innovation of Malaysia (MOSTI) for financial support.

#### References

- [1] C.T. Kresge, M.E. Leonowicz, W.J. Roth, J.C. Vartuli, J.S. Beck, *Nature* 359 (1992) 710.
- [2] Y. Sun, Y. Yue, Z. Gao, *Appl. Catal. A: Gen.* 161 (1997) 121.
- [3] X. Hu, G.K. Chuah, S. Jaenicke, *Appl. Catal. A: Gen.* 217 (2001) 1.
- [4] M. Selvaraj, P.K. Sinha, A. Pandurangan, *Micropor. Mesopor. Mater.* 70 (2004) 81.
- [5] M. Selvaraj, P.K. Sinha, K.S. Seshadri, A. Pandurangan, *Appl. Catal. A: Gen.* 265 (2004) 75–84.
- [6] M. Selvaraj, A. Pandurangan, K.S. Seshadri, P.K. Sinha, V. Krishnasamy, K.B. Lal, *J. Mol. Catal. A* 192 (2003) 153.
- [7] H. Nur, D. Prasetyoko, Z. Ramli, S. Endud, *Catal. Commun.* 5 (2004) 725.
- [8] N.E. Poh, H. Nur, M.N.M. Muhid, H. Hamdan, *Catal. Today* 114 (2006) 257.
- [9] G.D. Yadav, N.S. Doshi, *Appl. Catal. A: Gen.* 236 (2002) 129–147.

- [10] R. Savidha, A. Pandurangan, M. Palanichamy, V. Murugesan, *J. Mol. Catal. A: Chem.* 211 (2004) 165.
- [11] S.J. Wu, J.H. Huang, T.H. Wu, K. Song, H.S. Wang, L.H. Xing, H.Y. Xu, L. Xu, J.Q. Guan, Q.B. Kan, *Chin. J. Catal.* 27 (2006) 9.
- [12] K. Zhang, H.B. Zhang, G.H. Xu, S.H. Xiang, D. Xu, S.Y. Liu, H.X. Li, *Appl. Catal. A: Gen.* 207 (2001) 183.
- [13] K.U. Nandhini, B. Arabindoo, M. Palanichamy, V. Murugesan, *J. Mol. Catal. A: Chem.* 223 (2004) 201.
- [14] P. Selvam, S.E. Dapurkar, *Catal. Today* 96 (2004) 135.
- [15] T. Mathew, B.S. Rao, C.S. Gopinath, *J. Catal.* 222 (2004) 107.
- [16] M. Karthik, A.K. Tripathi, N.M. Gupta, A. Vinu, M. Hartmann, M. Palanichamy, V. Murugesan, *Appl. Catal. A: Gen.* 268 (2004) 139.
- [17] A.H. Padmasri, A. Venugopal, V.D. Kumari, K.S.R. Rao, P.K. Rao, *J. Mol. Catal. A: Chem.* 188 (2002) 255.
- [18] A. Sakthivel, S.K. Badamali, P. Selvam, *Micropor. Mesopor. Mater.* 39 (2000) 457–463.
- [19] R. Anand, R. Maheswari, K.U. Gore, B.B. Tope, *J. Mol. Catal. A: Chem.* 193 (2003) 251.
- [20] A.V. Krishnan, K. Ojha, N.C. Pradhan, *Org. Process Res. Dev.* 6 (2002) 132.
- [21] R.R. Mukti, M.Sc. Thesis, Universiti Teknologi Malaysia, Johor, Malaysia, 2003.
- [22] M. Kruk, M. Jaroniec, Y. Sakamoto, O. Terasaki, R. Ryoo, C.H. Ko, *J. Phys. Chem. B* 104 (2000) 294.
- [23] G. Leofanti, M. Padovan, G. Tozzola, B. Venturelli, *Catal. Today* 41 (1998) 207.
- [24] C.G. Sonwane, S.K. Bhatia, *J. Phys. Chem. B* 104 (2000) 9099.
- [25] C.N.R. Rao, *Chemical Applications of Infrared Spectroscopy*, Academic Press, New York, 1963.
- [26] J.T. Kloprogge, P.J.J. Dirken, B.H. Jansen, J.W. Geus, *J. Non-Cryst. Sol.* 181 (1995) 151.
- [27] J. Dwyer, *Zeolite Microporous Solids. Synthesis, Structure and Reactivity*, in: E.G. Derouane, F. Lemos, C. Naccache, F. Ribeiro (Eds.), NATO ASI Series, vol. 362, Kluwer, Dordrecht, 1992, p. 303.
- [28] Y. Marcus, *The Properties of Solvents*, John Wiley & Sons Ltd., New York, 1998.
- [29] A. Taguchi, F. Schüth, *Micropor. Mesopor. Mater.* 77 (2005) 1.